Paleoceanography and Paleoclimatology

RESEARCH ARTICLE
10.1029/2019PA003684

Coral Records of Temperature and Salinity in the Tropical Western Pacific Reveal Influence of the Pacific Decadal Oscillation Since the Late Nineteenth Century

R. D. Ramos[1], N. F. Goodkin[1,2], F. P. Siringan[3], and K. A. Hughen[4]

[1]Earth Observatory of Singapore, Nanyang Technological University, Singapore, [2]American Museum of Natural History, New York, NY, USA, [3]The Marine Science Institute, University of the Philippines-Diliman, Quezon City, Philippines, [4]Marine Chemistry and Geochemistry, Woods Hole Oceanographic Institution, Woods Hole, MA, USA

Abstract The Pacific Decadal Oscillation (PDO) is a complex aggregate of different atmospheric and oceanographic forcings spanning the extratropical and tropical Pacific. The PDO has widespread climatic and societal impacts, thus understanding the processes contributing to PDO variability is critical. Distinguishing PDO-related variability is particularly challenging in the tropical Pacific due to the dominance of the El Niño–Southern Oscillation and influence of anthropogenic warming signals. Century-long western Pacific records of subannual sea surface temperature (SST) and sea surface salinity (SSS), derived from coral Sr/Ca and $\delta^{18}O$ profiles, respectively, allow for evaluating different climatic sensitivities and identifying PDO-related variability in the region. The summer Sr/Ca-SST record provides evidence of a significant SST increase, likely tied to greenhouse gas emissions. Anthropogenic warming is masked in the winter Sr/Ca-SST record by interannual to multidecadal scale changes driven by the East-Asian Winter Monsoon and the PDO. Decadal climate variability during winter is strongly correlated to the PDO, in agreement with other PDO records in the region. The PDO also exerts influence on the SSS difference between the dry and wet season coral $\delta^{18}O$ ($\delta^{18}O_c$)-SSS records through water advection. The PDO and El Niño–Southern Oscillation constructively combine to enhance/reduce advection of saline Kuroshio waters at our site. Overall, we are able to demonstrate that climate records from a tropical reef environment significantly capture PDO variability and related changes over the period of a century. This implies that the tropical western Pacific is a key site in understanding multifrequency climate variability, including its impact on tropical climate at longer timescales.

Key Points:
- Palaui wintertime SST variability is sensitive to the Pacific Decadal Oscillation
- The Pacific Decadal Oscillation exerts influence on the salinity variability in Palaui
- The tropical western Pacific is a key site in understanding multifrequency climate variability

Supporting Information:
- Supporting Information S1
- Data Set S1

Correspondence to:
R. D. Ramos,
rramos@ntu.edu.sg

Citation:
Ramos, R. D., Goodkin, N. F., Siringan, F. P., & Hughen, K. A. (2019). Coral records of temperature and salinity in the tropical western Pacific reveal influence of the Pacific Decadal Oscillation since the late nineteenth century. *Paleoceanography and Paleoclimatology*, *34*, 1344–1358. https://doi.org/10.1029/2019PA003684

Received 2 JUN 2019
Accepted 30 JUL 2019
Accepted article online 5 AUG 2019
Published online 17 AUG 2019

1. Introduction

The Pacific Decadal Oscillation (PDO) is the dominant mode of sea surface temperature (SST) anomalies over the North Pacific poleward of 20°N at decadal timescales (Mantua et al., 1997; Mantua & Hare, 2002). The PDO rapidly transitions between prolonged periods of warm (positive) and cold (negative) phases every few decades (Mantua et al., 1997; Minobe, 1997; Newman et al., 2016), altering rainfall patterns and ocean productivity in the region. During warm (positive) PDO phases, SSTs are anomalously warm along the northwest coast of North America, coincident with increased rainfall along the coast including the southwest United States and Central America, and decreased rainfall and streamflow in the interior western United States (Felis et al., 2010; Mantua & Hare, 2002; Miller et al., 1994; Nigam et al., 1999). Over the western and central Pacific, SSTs are anomalously cooler, coincident with decreased rainfall in the western Pacific and increased extratropical storm intensities in the northwestern Pacific (Felis et al., 2010; Mantua & Hare, 2002; Miller et al., 1994). The SST anomalies and precipitation impacts reverse during a cold (negative) PDO phase (Felis et al., 2010; Mantua & Hare, 2002). Changes in ocean productivity in Alaska and the western coast of the United States are correlated with the phase shifts of the PDO, significantly impacting marine ecosystems and fishing industries (Mantua et al., 1997; Overland et al., 2008). While less constrained, the PDO's influence extends to the tropics (Newman et al., 2016). The PDO interacts with the interannually dominant El Niño–Southern Oscillation (ENSO) in the tropics resulting in decadal SST and sea surface salinity (SSS) trends being broadly similar to ENSO patterns (Delcroix et al., 2007; Deser et al., 2004). The PDO also influences the Asian monsoon system by modulating the response of the East Asian winter monsoon (EAWM) to ENSO (e.g., Kim et al., 2014; L. Wang et al., 2008). Understanding the mechanisms driving PDO variability is therefore critical to the mitigation of its impacts and their predictability in the future.

More than just a single mode of climate variability, the PDO is presently considered a combination of extratropical and tropical atmospheric and oceanographic processes operating at varying timescales (Liu & Di Lorenzo, 2018; Newman et al., 2016). The strength of the Aleutian Low, persistent oceanic memory closely dependent on ENSO-SST anomalies, and the Kuroshio Current system act together to drive the spatial pattern of the PDO (Newman et al., 2016). Each PDO shift may then be a result of different combinations of the above processes (Deser et al., 2004; Newman et al., 2016), confounding our understanding of its climatic behavior. Adding more complexity in constraining decadal variability is anthropogenic warming, where the shift of the PDO in 1976–1977 from cold to warm phase is hypothesized to be linked to greenhouse gas emissions (Cole et al., 2000; Graham, 1995; Miller et al., 1994; Nurhati et al., 2011). One approach to overcome these challenges is to document the different processes that contribute to PDO variability beyond the instrumental period and anthropogenic influence, allowing identification of dependent and independent forcing mechanisms of the PDO and how their interrelationships varied back in time (Newman et al., 2016).

Networks of tree-ring records from continental East Asia and northwestern America provide multicentury to millennial scale histories of PDO variability (e.g., Biondi et al., 2001; D'Arrigo & Wilson, 2006; Gedalof & Smith, 2001; MacDonald & Case, 2005; Minobe, 1997). However, terrestrial data do not fully represent oceanic processes linked to the PDO. Coral-based records documenting interannual to multidecadal SST patterns are concentrated in the central and south Pacific regions (e.g., Cobb et al., 2001; Linsley et al., 2000; Nurhati et al., 2011; Urban et al., 2000) but are extremely rare in the tropical and subtropical western Pacific (e.g., Asami et al., 2005; Felis et al., 2010). Most of these records are based on $\delta^{18}O$ profiles, preventing independent estimates of SST anomalies in the region. Because the PDO is an aggregate of several processes and remotely influences the ENSO-dominated tropical region, combined records of Sr/Ca and $\delta^{18}O$ are more advantageous to accurately estimate PDO-related climate variability.

A previous study using corals from Palaui, northeastern Luzon, Philippines (Ramos et al., 2017), shows that interspecies (i.e., averaged *Diploastrea heliopora* and *Porites lobata*) wintertime Sr/Ca-SST is sensitive to PDO variability, providing support for PDO reconstruction at longer timescales. It was also shown that the *P. lobata* dry (winter) season $\delta^{18}O_c$-SSS record, compared with that of the wet (summer) season, reflects regional changes in salinity, allowing for a reconstruction of ENSO variability. In this paper, we present extended records of Sr/Ca and $\delta^{18}O$ proxies derived from the same *P. lobata* core and reconstructed SST and SSS for the past ~132 years using previously published *P. lobata* proxy calibrations (Ramos et al., 2017). We assess these records across different frequencies to examine their relative sensitivity to PDO variability and possible changes in these relationships through time. We also evaluate the potential impacts of the PDO on tropical western Pacific climate, which is considered to weakly correspond to decadal climate variability (Deser et al., 2004; Mantua & Hare, 2002; Newman et al., 2016).

2. Coral Sampling and Analytical Methods

In May 2012, a 3-m long coral core of *Porites lobata* was collected from 4- to 5-m water depth off the coast of Palaui Island, Philippines (18.5°N, 122.2°E; Figure 1). The core was drilled using a pneumatic drill with ~55-mm diameter core bit. Monthly instrumental SST (Integrated Global Ocean Services System, centered at 18.5°N, 122.5°E; Reynolds et al., 2002) and SSS (Simple Ocean Data Assimilation, centered at 18.8°N, 122.3°E; Carton & Giese, 2008) records from 1982 to 2012 indicate that the warmest and wettest months occur from June to September while the coldest and driest months occur from December to March. Mean annual SST and SSS both exhibit limited variability (i.e., 1.4°C and 0.66 psu, respectively). Annual rainfall is on average 2,000 ± 500 mm/year (1σ; Philippine Atmospheric Geophysical and Astronomical Services Administration).

Palaui Island is located at the northeastern tip of Luzon facing the western Pacific Ocean to its east and the Luzon Strait to its north. It lies near the northern tip of the western Pacific warm pool where the Asian monsoon, ENSO and the PDO exert influences on the regional SST, salinity, and rainfall variability at seasonal to multidecadal timescales (e.g., Delcroix et al., 2007; H. Wang & Mehta, 2008; Yan et al., 1992).

2.1. Coral Subsampling

The coral core was cleaned, cut into 7-mm thick slabs, and X-rayed according to methods previously outlined (Ramos et al., 2017). Using a micrometer-controlled drill press, subsamples were drilled along the extending

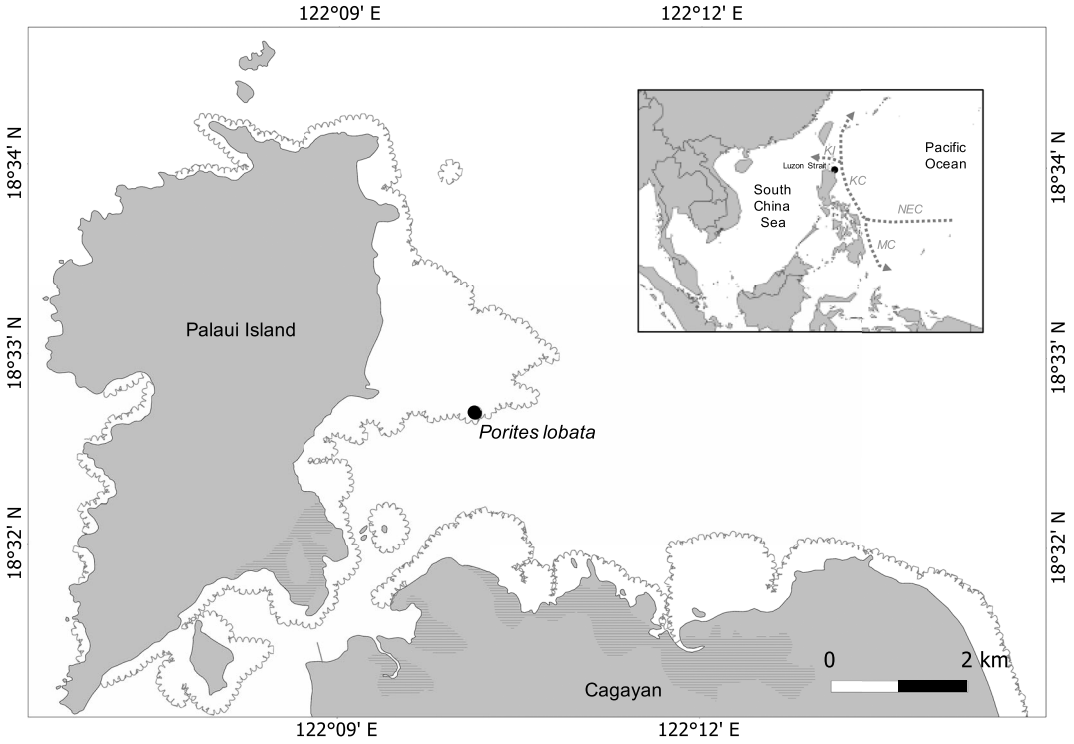

Figure 1. A coral core of *Porites lobata* was drilled offshore Palaui island in May 2012. Palaui island is located at the northeastern tip of Luzon (black dot), Philippines, facing the Luzon Strait and the Pacific Ocean (inset). Dashed lines delineate major currents, NEC = North Equatorial Current; MC = Mindanao Current; KC = Kuroshio Current; KI = Kuroshio Intrusion.

corallites at 0.5-mm increments and at constant sampling depth of 1 mm, yielding approximately biweekly sampling resolution. Each individual sample weighed <300 μg and 40- to 90-μg powder splits were set aside for stable isotope analysis. The remaining powder was used for Sr/Ca measurements.

2.2. Sr/Ca Analysis

Approximately 200 μg of subsample was dissolved in 2.5 mL of 5% HNO_3 overnight. Sr and Ca were simultaneously measured thrice per sample using an inductively coupled plasma-optical emission spectrometer (Thermo iCAP 6000 Series) at the Asian School of the Environment, Nanyang Technological University. Solution standards (0 to 80 ppm) were routinely measured to correct for instrumental drift and matrix effects from varying calcium concentrations (Schrag, 1999). Bulk coral powder reference material JCp-1 (Okai et al., 2001) with a consensus Sr/Ca value of 0.01932 (±0.0002) ppm or 8.838 (±0.089) mmol/mol (Hathorne et al., 2013) and an in-house powder standard (*Porites* sp.) were both analyzed throughout each run to evaluate measurement precision. Repeat measurements of JCp-1 and the in-house coral powder standard analyzed over a period of 2 years showed very good reproducibility, 0.019291 (±0.00004) ppm or 8.824 (±0.018) mmol/mol (1σ, relative standard deviation = 0.18%, n = 1074) and 0.019289 (±0.00005) ppm or 8.823 (±0.023) mmol/mol (1σ, relative standard deviation = 0.25%, n = 396), respectively.

2.3. $\delta^{18}O$ Analysis

Oxygen stable isotope ratios, $\delta^{18}O$, were analyzed in an automated Kiel IV carbonate device coupled with a ThermoFisher MAT-253 isotope ratio mass spectrometer and on a Thermo-Finnigan Delta V Advantage isotope ratio mass spectrometer with Gasbench (GB) II, both at Asian School of the Environment, Nanyang Technological University. Powdered samples were acidified with 105% H_3PO_4 at 70 °C. Measurements were calibrated relative to Vienna Peedee belemnite using external standards including National Bureau of Standards (NBS) 19 ($\delta^{18}O$ = 2.20‰) and NBS 18 ($\delta^{18}O$ = 23.2‰; Stichler, 1995). Repeat measurements of NBS 19 and marble standard, Estremoz ($\delta^{18}O = -5.95 \pm 0.07$‰), on Delta V-GB II yield a precision of ±0.06‰ (1σ, n =6) and ±0.08‰ (1σ, n =12), respectively, consistent with that of the

Kiel IV-MAT 253 analyzed over a 2-year period ($\delta^{18}O_{NBS\ 19} = \pm 0.07‰$, 1σ, $n = 103$; $\delta^{18}O_{Estremoz} = \pm 0.08‰$, 1σ, $n = 1{,}294$). These carbonate standards yield comparable results on both mass spectrometers with $\delta^{18}O_{NBS\ 19}$ showing a slight enrichment on the Delta V-GB II (mean difference of −0.08‰ and 0.07‰ for $\delta^{18}O_{NBS\ 19}$ and $\delta^{18}O_{Estremoz}$, respectively; $n = 18$). However, the average enrichment is statistically insignificant and less than 25% of the monthly $\delta^{18}O$ variability, unlikely to introduce a bias between samples analyzed on the Delta V-GB II (i.e., wet season samples prior to 1894) and Kiel IV-MAT 253 (i.e., monthly samples from 1894 to 2012 and dry season samples prior to 1894).

Prior to 1894, $\delta^{18}O$ was only measured on dry and wet season samples. The dry (wet) $\delta^{18}O$ samples were selected on the basis of the winter (summer)-time Sr/Ca depth- and time-series data, in which $\delta^{18}O$ and Sr/Ca maxima (minima) coincide seasonally. Each season constitutes about four to eight consecutive $\delta^{18}O$ samples, representing the dry and wet season values of each year. The reduction in sample points and the difference in instrumentation are unlikely to create a bias across time periods as we consistently examine seasonal extremes at interannual to multidecadal timescales. Time assignments for the interannual dry and wet season $\delta^{18}O$ followed that of the paired Sr/Ca data.

2.4. Chronology Development

Age-depth models were developed using the annual density bands (supporting information Figure S1 in the supporting information) and fine-tuned using the seasonal cycles of Sr/Ca. Beyond the instrumental and calibration period (i.e., 1982 to 2012) previously reported (Ramos et al., 2017), ages were assigned using the averaged Integrated Global Ocean Services System SST climatology, aligning Sr/Ca profile minima, maxima, and inflection points with their respective SST points each year using the Analyseries software (Paillard et al., 1996). The Sr/Ca time series was then linearly interpolated into a monthly record. The rough Sr/Ca-SST age-depth model was similarly applied to the corresponding $\delta^{18}O$ record, which was then interpolated at monthly resolution.

2.5. SST and SSS Reconstruction

Records of SST and SSS variability extending back to 1880 were reconstructed using previously published calibration equations for SST:

$$\begin{gathered} \mathrm{Sr/Ca} = 10.790\ (\pm 0.043) - 0.068\ (\pm 0.002) \times \mathrm{SST}\ (°\mathrm{C}) \\ r = -0.92, p < 0.0001, \mathrm{RMSR} = 0.61°\mathrm{C}, n = 377 \end{gathered} \tag{1}$$

and SSS:

$$\begin{gathered} \delta^{18}O_{c\_3yr\_wet\&dry} = -41.722\ (\pm 3.792) - 1.075\ (\pm 0.111) \times SSS_{3yr\_wet\&dry}\ (\mathrm{psu}) \\ r = 0.93, p < 0.0001, \mathrm{RMSR} = 0.09\ \mathrm{psu}, n = 18 \end{gathered} \tag{2}$$

(Ramos et al., 2017), where RMSR is the root-mean-square of the residual describing the difference between the instrumental and reconstructed records. These equations were applied to interannual reconstructions (i.e., summer/3-year wet and winter/3-year dry SST and SSS) to effectively increase the signal to noise ratio that may otherwise be dampened by the limited SST and SSS variability at our site (Ramos et al., 2017).

2.6. Data Analysis

We estimated the power spectral density on our records and climate indices using a simple fast Fourier transform (FFT) algorithm. Significance level (90%) was estimated using 10,000 Monte Carlo simulations. We also performed coherence and phase analysis using a nonparametric multitaper method (MTM) with bias correction (https://www.mathworks.com/matlabcentral/fileexchange/22551-multi-taper-coherence-method-with-bias-correction; Huybers & Denton, 2008) to evaluate the significant frequencies shared by our reconstructions and climate indices. MTM coherence was estimated with two windows and 50 iterations on Monte Carlo error estimates. To further isolate and observe variability specific to coherent frequencies between records, we applied a Gaussian filter using the Analyseries software (Paillard et al., 1996).

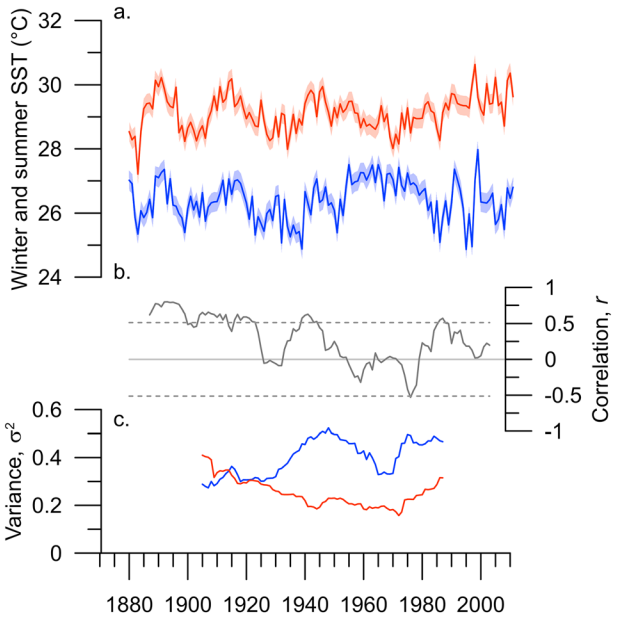

Figure 2. (a) Interannual summer (red) and winter (blue) Sr/Ca-SST reconstructions. Shading represents RMSR = 0.61 °C. (b) Fifteen-year running correlation between the summer and winter SSTs record. Dashed line represents 95% significance level. (c) Fifty-year running variance of summer (red) and winter (blue) SSTs.

3. Results

3.1. Sr/Ca–SST Reconstruction

The Sr/Ca record shows distinct annual cycles throughout the reconstruction period extending back to 1880 (Data Set S1 and Figure S2 in the supporting information). The summer and winter SST reconstructions exhibit interannual to multidecadal scale variability over a 3.4 and 3.1 °C SST range, respectively (Figure 2a). Both interannual reconstructions show similar trends at the beginning of the record, indicated by their significant positive 15-year running correlation (Figure 2b). Around the mid-1920s, the records decouple, with negligible relationships recorded during 1925–1935, 1947–1974, 1979–1983, and 1994–2012. This change in decadal behavior between records through time is confirmed by calculating the 50-year running variance for each record (Figure 2c). Summer SST exhibits a gradual decrease in variance that reverses in direction in the early 1970s. Winter SST shows similar variance to that of the summer record until the late 1920s when it began to steeply increase, reaching a peak around 1950 (Figure 2c). The winter SST variance subsequently decreased until the mid-1960s when variance increased to the previous magnitude (Figure 2c). There is no discernible long-term trend in either SST record ($m_{summerSST}$ = 0.0029 °C/year and $m_{winterSST}$ = 0.0014 °C/year; $r < 0.2$, $p < 0.05$), indicating minimal mean SST change over the past century. However, from 1970 to present, the summer record shows an SST increase of 0.03 °C/year or 1.23 °C over the past ~4 decades ($r = 0.66$, $p < 0.0001$), indicating significant recent summer warming.

3.1.1. Evaluating Drivers of SST Variability

The PDO has previously been shown to exert an influence on Palaui winter SST variability, with warm (positive) PDO events characterized by anomalously cool SSTs in the western Pacific and central North Pacific Ocean (Felis et al., 2010; Gedalof & Smith, 2001; Mantua et al., 1997; Ramos et al., 2017). The extended winter SST record reported here exhibits significant correlation with the PDO at both interannual ($r = -0.34$, $p < 0.0001$, $n = 112$) and 3-year binned timescales ($r = -0.55$, $p < 0.001$, $n = 38$) from 1880 to 2012. Compared with other modes of Pacific decadal variability (i.e., Interdecadal Pacific Oscillation, IPO (Power et al., 1999), and North Pacific Index, NPI (Trenberth & Hurrell, 1994)), our winter SST record is weakly correlated ($r_{IPO} = -0.01$ and $r_{NPI} = 0.10$, $p > 0.30$). This suggests that interannual to multidecadal SST changes in our winter SST reconstruction may strongly be linked to the PDO.

To further evaluate the robustness of this relationship and quantify the significant frequencies shared between our coral records and climate indices, we generated MTM power spectral densities and coherence between our summer and winter SST reconstructions and the PDO index over the same time period between 1901 and 2010. We similarly performed this analysis using solar irradiance (Lean, 2000), ENSO (i.e., Niño 3.4) and EAWM (D'Arrigo et al., 2005) indices over the same time period for comparison to the SST records.

Results of the FFT spectral analysis reveal significant variance at multidecadal periods of 55 years/cycle and interannual periods of 3.1–3.2 and 2.1–2.3 years/cycle in the winter SST record and the PDO index (Figures 3a and 3b.1). Further evidence that our record is sensitive to the PDO is spectral coherence (>90%) at the previously mentioned frequencies and at periods of ~10 years/cycle (Figure 3b.2). Between the winter SST and the EAWM, the records show significant power and coherence at a period of 2.8 years/cycle (Figure 3c.2), indicating the additional influence of the EAWM on the winter SST variability at high frequencies. The winter SST also reveals significant spectral power at interannual periods of 2.6 and 3.7 years/cycle (Figure 3a) but is incoherent with the Niño 3.4 index and solar irradiance (supporting information Figure S2).

Summer SST, on the other hand, exhibits significant power at 2.3, 2.5, 3.7, and 5.2 years/cycle (supporting information Figure S3). Compared with the PDO, EAWM, and Niño 3.4 indices and solar irradiance (supporting information Figure S3), summer SST is incoherent with these records at the previously

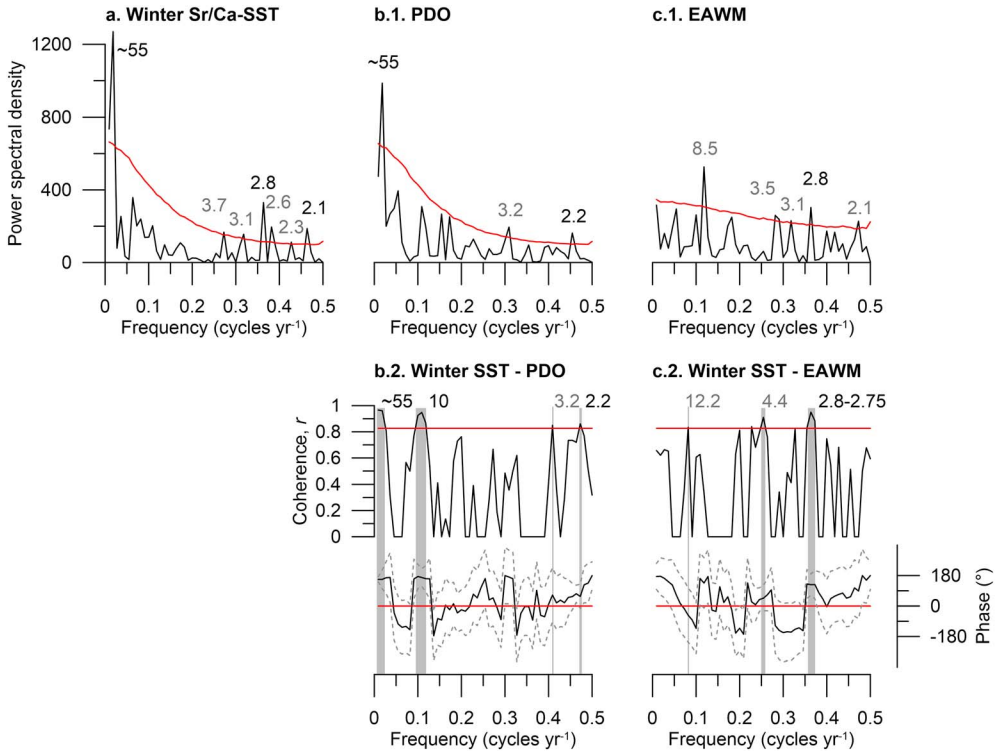

Figure 3. FFT (upper panel) analysis of (a) detrended winter Sr/Ca-SST records and climate indices, (b.1) PDO and (c.1) EAWM. Significance level greater than 90% (red lines) are labelled. Coherence multitaper method with phase analysis (lower panel) is also performed to account for variances shared between (b.2) winter SST and the PDO and (c.2) winter SST and EAWM indices. Red lines indicate 90% significance level while the gray dashed lines represent confidence intervals. Black labels are the periods further analyzed. SST = sea surface temperature; PDO = Pacific Decadal Oscillation; EAWM = East Asian winter monsoon.

mentioned time frequencies, indicating that the impact of these climatic forces on the summer SST record is limited or absent. Therefore, we further investigate the drivers of multifrequency SST variability focusing on the winter SST reconstruction and the PDO and EAWM indices.

3.1.2. Palaui Winter SST Variability

The winter SST record and EAWM indices were filtered to 0.359 ± 0.0045 cycles/year (2.8 year/cycle). The SST and PDO records were filtered to 0.018 ± 0.0045 (55 years/cycle), 0.105 ± 0.0045 (10 years/cycle) and 0.473 ± 0.0045 (2.1 years/cycle) cycles/year.

The 2.8-year filtered winter SST and EAWM records show a significant negative correlation ($r = -0.43$, $p < 0.0001$; Figures 4a and 4b), consistent with regional cooling during strong EAWM periods. The relatively low correlation strength between records is likely due to the change in sign through time, only showing significant negative relationships around the mid-1960s toward the present (Figure 4b). The observed gradual increase in amplitude in the EAWM record reaching maximum values in the 1960s is not evident in our winter SST reconstruction but may explain the change in phase and correlation strength between records, which occurred about the same time.

The 2.1-year filtered winter SST and PDO records show a significant but low negative correlation ($r = -0.30$, $p = 0.002$; Figures 4c and 4d), likely resulting from the observed change in phase over time. Changes in phase are not observed in the 10- and 55-year filtered records, which in contrast exhibit strong antiphase relationships ($r_{10\text{-}year} = -0.96$ and $r_{55\text{-}year} = -0.90$, $p < 0.0001$; Figures 5a and 5b), consistent with the known spatial structure of the PDO-related SST anomalies across the Pacific. The 55-year filtered timeseries reveal consistent amplitudes throughout the records (Figure 5a), whereas in the 10-year filtered timeseries, the amplitudes were attenuated between 1920 and 1940 and became gradually amplified toward the present (Figure 5b), suggesting a more active PDO in recent years. On the basis of these results, we

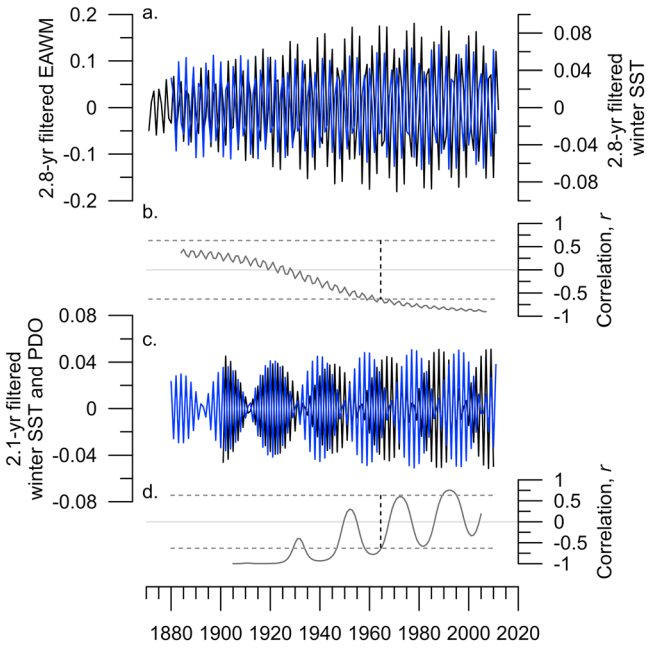

Figure 4. (a) The 2.8-year filtered winter SST (blue) and EAWM record (black). (b) The 10-year running correlation reveals significant relationship from early the 1960s. Horizontal dashed lines represent 95% significance level. (c and d) The same as (a and b) but for the 2.1-year filtered winter SST and PDO records. Vertical dashed lines indicate the time when the PDO and EAWM inversely modulates SST variability. SST = sea surface temperature; PDO = Pacific Decadal Oscillation; EAWM = East Asian winter monsoon.

applied a 10-year moving average on the winter SST record to reconstruct the winter PDO (Figure 5c). Compared with the similarly averaged PDO index, the records show a strong negative relationship ($r = -0.75$, $p < 0.0001$, $n = 101$; Figure 5c), highlighting that SST variability at this site reliably records the PDO at decadal scale.

Our winter SST record exhibits known regime shifts since the start of the twentieth century: shifts from cold to warm phase in 1924 and 1976 and shifts from warm to cold phase in 1945 and 1998 (Figure 5c). Beyond 1900, when the PDO index is no longer available, we find good agreement ($r = 0.77$, $p < 0.0001$) in the SST fluctuations between our record and the only available coral Sr/Ca-based PDO reconstruction in the western Pacific, Ogasawara coral from southern Japan (Felis et al., 2010; Figure 5d). Both coral records exhibit warm winter SST anomalies between 1885 and 1895 (Figures 5c and 5d), indicative of a cold (negative) PDO phase during this period. While the climatological winter SST averages were slightly different for Palaui and Ogasawara (i.e., December to March and November to February, respectively), the two coral records exhibit good overall reproducibility ($r = 0.50$, $p < 0.0001$, $n = 106$) over 10-year timescales, suggesting that the two proxy reconstructions from different geographical locations are responding to the same decadal forcing.

3.2. Dry and Wet season $\delta^{18}O_c$-SSS Reconstruction

Similar to the Sr/Ca record, the $\delta^{18}O$ record was extended back to 1880 (Data Set S1 and Figures S2and S3/> in the supporting information), allowing for interannual dry and wet SSS reconstructions. The interannual salinity reconstructions show distinct patterns (Figure 6a) with the dry season $\delta^{18}O_c$-SSS varying between 34.2 and 34.9 psu, with a range of 0.76 psu. The wet season $\delta^{18}O_c$-SSS, on the other hand, varies between 33.8 and 34.7 psu, showing a slightly higher range than the dry season record, 0.91 psu.

Since the late nineteenth century, the dry season SSS record exhibits a long-term decreasing trend of 0.003 psu/year ($r^2 = 0.52$, $p < 0.0001$; Figure 6a), indicative of freshening. Wet season SSS shows no observable long-term trend (slope, $m_{wet(1880–2012)} = -0.0020$ psu/year), but a "drier" anomaly is observed during the late nineteenth century and during a prolonged period between 1950 and 1980. Around 1976 to present, the wet season SSS record decreased to similar magnitude prior to the prolonged drier period, indicative of recent freshening.

While the seasonal salinity variations appear independent, there are periods when the salinity values in both seasons are statistically equivalent. Between 1958 and 1976, the salinity difference between the dry and wet season SSS records is small to negligible (<0.15 psu; Figure 6b), indicating the loss of SSS seasonality. Before and after this time period, the salinity difference is greater than 0.15psu, reaching a maximum of 0.72psu in the early 1930s (Figure 6b). The similarity in SSS values between 1958 and 1976 could be due to seasonal excursions resulting from offsets in timing between ENSO or local rainfall at our site as previously reported (Ramos et al., 2017). However, at longer timescales the SSS difference shows distinct decadal variability that we hypothesize is additionally controlled by large-scale processes.

3.2.1. Evaluating Drivers of SSS Variability

To evaluate the controlling factors in the seasonal SSS reconstructions at longer time periods, we compared the SSS difference to the PDO index. The PDO is significantly correlated to the dry-wet season SSS difference ($r = 0.39$, $p = 0.02$, $n = 37$; Figure 6b) such that the period of small SSS seasonality coincides with the predominant cold (negative) PDO phase, while periods of larger SSS differences coincide with the predominant warm (positive) PDO phases. The correlation becomes stronger and more significant with application of a 3- and 6-year lag on the PDO time series ($r_{3yr\_lag} = 0.57$, $p < 0.0001$, $n = 36$ and $r_{6yr\_lag} = 0.72$, $p < 0.0001$, $n = 35$), providing further support that the PDO exerts influence on the SSS variability at our site.

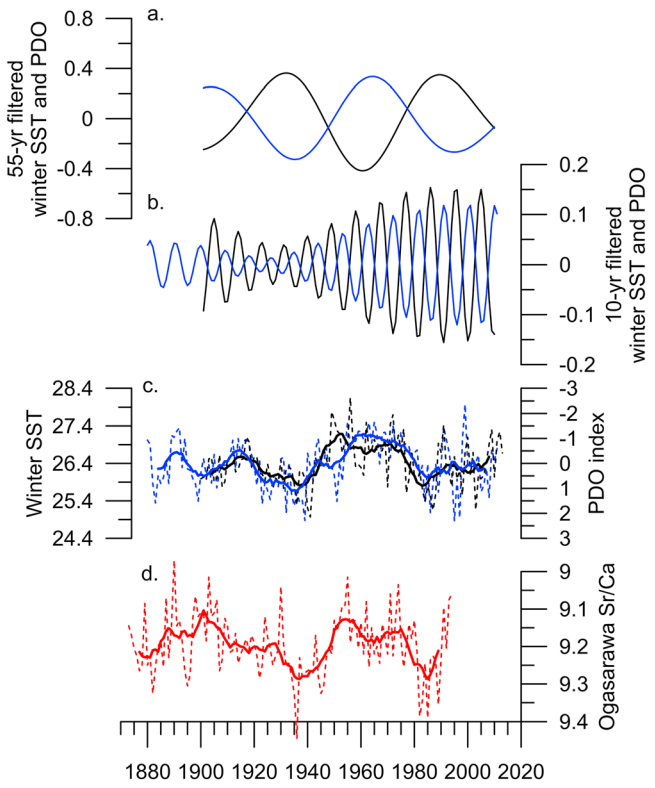

Figure 5. The (a) 55- and (b) 10-year-filtered winter SST (blue) and PDO index (black). (c) Interannual (dashed) and 10-year moving averaged (solid) winter SST reconstruction (blue) compared to the PDO (black) and (d) interannual (dashed) and 10-year moving averaged (solid) coral Sr/Ca record from Ogasawara, Japan (red; Felis et al., 2010). SST = sea surface temperature; PDO = Pacific Decadal Oscillation.

Results of the spectral analysis reveal significant power at periods of 6.8 and 6.4 years/cycle in the SSS difference and PDO records, respectively (Figure 7a). In addition, both records are significantly coherent at periods >27 years/cycle (Figure 7b). Because we are interested in low frequency variability, we filtered our data to 0.023 ± 0.014 cycle/year. The >27-year filtered records show a strong positive relationship, despite the PDO leading by 6 years ($r = 0.70$, $p < 0.0001$, $n = 37$; Figure 7c). Accounting for this lead results in a stronger positive relationship ($r = 0.96$, $p < 0.0001$, $n = 35$), suggesting a significant PDO-related control on salinity variability at longer timescales.

4. Discussion

4.1. Climatic Controls on SST Variability

Both the summer and winter Sr/Ca-SST records capture SST variability significantly, each providing records of different SST behaviors. Our SST reconstructions are significantly correlated at the beginning of the records until the mid-1940s (Figure 2b), suggesting that seasonal SST changes are governed by similar factors. However, toward the present, the summer SST record indicates a significant warming trend that started in the 1970s (Figures 2a and 8a), whereas the winter SST record shows a different response (Figure 2a). Beginning in the 1970s, both records exhibits increasing variance (Figure 2c). However, the winter SST variance is consistent with decadal scale changes in variance throughout the record, whereas summer SST variance only had a decreasing trend earlier in the record before 1970. The onset of increasing summer SSTs (Figure 8a) is coincident with the onset of regional warming (e.g., Tierney et al., 2015 and references therein) likely tied to increasing anthropogenic greenhouse gas emissions during this period. A record of well-mixed greenhouse gas-radiative forcing (Schmidt et al., 2012) indicates that its magnitude over the most recent 50 years increased thrice as fast compared to the preceding 50 years (i.e., 1950 to 2000: 0.0270 W m^{-2} $year^{-1}$ [$r^2 = 0.99$, $p < 0.0001$] vs. 1900 to 1950: 0.0094 W m^{-2} $year^{-1}$ [$r^2 = 0.99$, $p < 0.0001$]; Figure 8b). However, compared to the magnitude of a 1° by 1° gridded instrumental summer SST record at our site (i.e., 0.17 °C per decade; Rayner et al., 2003), our warming estimate is twice as high. This disagreement in magnitude may be due to differences in spatial coverage of the instrumental and proxy records where the latter better represents summer SST variability within a shallow reef environment. The presence of anthropogenic warming only in the more recent summer records, and not in the winter (as discussed below), may indicate the power of decadal scale variability in masking or slowing down anthropogenic signals in our SST records. One possible implication for this is that nonwarming winters may lessen the impacts of increased thermal stress in warming seas.

Winter SST exhibits greater sensitivity to the PDO- and EAWM-related SST changes. Interannual to multidecadal scale variability (i.e., 50 to 70 years) is a known feature of climatic oscillations in the North Pacific during the eighteenth and nineteenth centuries (Mantua & Hare, 2002). Multidecadal scale oscillations are present in coral records from Ogasawara (Felis et al., 2010) and Koshiki (Watanabe et al., 2014) islands in Japan, reflecting PDO variability in their SST (Sr/Ca) and summer monsoon ($\delta^{18}O$) reconstructions, respectively. Other marine-based North Pacific SST reconstructions including those extracted from coralline algae proxies (e.g., $\delta^{18}O$ (Halfar et al., 2007) and Mg/Ca (Williams et al., 2017)) and geoduck clam growth indices (e.g., Black et al., 2009; Strom et al., 2004; supporting information Figure S6) also exhibit multidecadal scale variability. Tree-ring climate reconstructions from continental East Asia, west Canada, and northwest America (e.g., Black et al., 2009; D'Arrigo & Wilson, 2006; MacDonald & Case, 2005; Minobe, 1997) also exhibit strong periodicities of 50 to 70 years. Causes of such multidecadal scale variability are still unclear (MacDonald & Case, 2005; Mantua & Hare, 2002) but are likely forced by ocean-atmosphere interaction and modulated by solar radiation (Minobe, 1997).

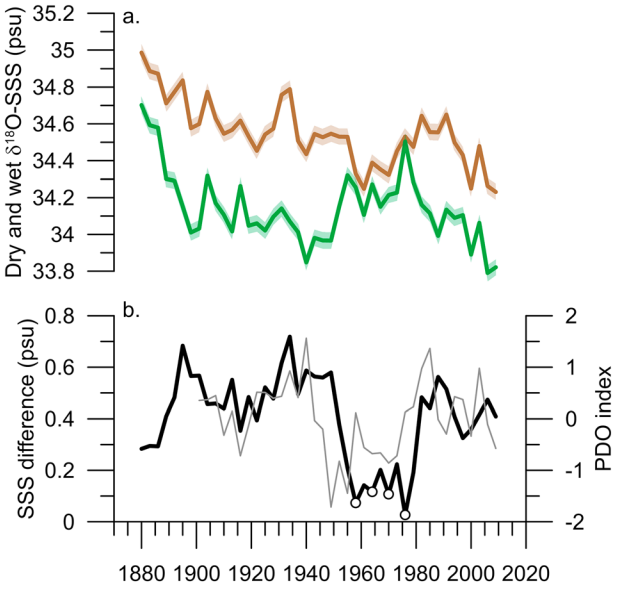

Figure 6. (a) Reconstructed dry (brown) and wet (green) season $\delta^{18}O_c$-SSS. Brown and green shading indicate RMSR = 0.09 psu. (b) SSS difference between the dry and wet season salinity records (thick black line) is significantly correlated to the PDO with 0 ($p = 0.02$, solid gray line) to 6-year lag ($p < 0.0001$, not shown). Hollow circles indicate times when the dry and wet season SSS values are statistically equivalent. Significant difference was calculated by propagating the reconstruction errors between the SSS records. SSS = sea surface salinity; PDO = Pacific Decadal Oscillation.

To compare the spatiotemporal behavior of the PDO, we applied a 55-year Gaussian filter (0.018 ± 0.0045 cycle/year) on the above PDO reconstructions (excluding the non-SST-related record from Koshiki). Our winter SST record shows strong correlations with the PDO index and both marine- and terrestrial-based reconstructions across the Pacific, showing the expected phase relationship (Table 1 and Figure 9). Significant but relatively weak correlations, on the other hand, are observed between the western and northern Pacific records and the strongly correlated records from northwest America and Canada (Table 1 and Figure 9). Due to the clustering of strong relationships between different proxies within a geographic area, but reduced correlations across regions, a change in the spatial pattern of the PDO over time is a likely cause. Because the PDO is a sum of several atmospheric and oceanic processes that are spatiotemporally dynamic (Newman et al., 2016), the observed inconsistency between regions can be expected as proxy sensitivity changes with location (D'Arrigo & Wilson, 2006; Newman et al., 2016). Reduced correlations to the PDO may also lead to increased proxy sensitivity to other local climatic or environmental influences such as ENSO, monsoon failures, volcanic eruptions, storm activity, and other extreme events, resulting in disagreement between records (e.g., D'Arrigo & Wilson, 2006; Williams et al., 2017). Nonetheless, good reproducibility between proxies within each region is valuable for understanding the processes that contribute to PDO variability.

Interannual oscillations observed in the western Pacific PDO records likely originate from ENSO signals known to imprint PDO variability (D'Arrigo & Wilson, 2006; Felis et al., 2010; Watanabe et al., 2014). However, coherence between our SST records and Niño 3.4 is absent. The interannual frequency of the EAWM is evident in our record but changes in its phase and amplitude are not reflected in our reconstruction, resulting in an obscured winter SST and EAWM relationship. This may be due to the strong multidecadal component driving our SST variability and masking the interannual signals. Comparing the high-frequency filtered winter SST, PDO, and EAWM records shows that the period of negligible relationship between winter SST and PDO coincides with the period when the EAWM influence on winter SST is more significant (Figure 4). Because the PDO and EAWM impact SSTs at our site in the same direction (i.e., positive PDO and positive EAWM leads to cooler SST anomalies at our site), it can be hypothesized that at different time periods, these climate systems may show dominance over the other in modulating SST variability at higher frequencies. Longer records are needed to verify these changes and formulate mechanisms describing the inter-relationship between the PDO and EAWM back in time.

4.2. Climate Controls of SSS Variability

The PDO impacts surface salinity at our site by modifying the hydrological balance (i.e., evaporation/precipitation) and/or water advection (Delcroix et al., 2007). During warm (cold) PDO phases, in situ salinity observations over the tropical Pacific indicate higher (lower) salinity values in the western Pacific due to decreased (increased) rainfall (Delcroix et al., 2007). However, we found the opposite relationship between the PDO and salinity reconstructions during the wet season at our site when maximum annual rainfall occurs. This suggests that the PDO dominantly impacts the seasonal SSS difference through water advection instead of precipitation. The Kuroshio current, a northward flowing western boundary current in the Pacific, transports high salinity western Pacific water to our site as it impinges on the coast and intrudes into the Luzon Strait (Hu et al., 2015; Nan et al., 2015; Qu et al., 1998). During warm (positive) PDO phases, the Kuroshio transport is slower, increasing Kuroshio intrusion into the Luzon Strait (Wu, 2013) and advecting more saline western Pacific waters to Palaui. Similarly, El Niño/La Niña events enhance/reduce Kuroshio intrusion into the strait (Qu et al., 2004; Ramos et al., 2019). Changes in Kuroshio transport are more pronounced during the winter (dry) season when ENSO events mature and prominent PDOs are

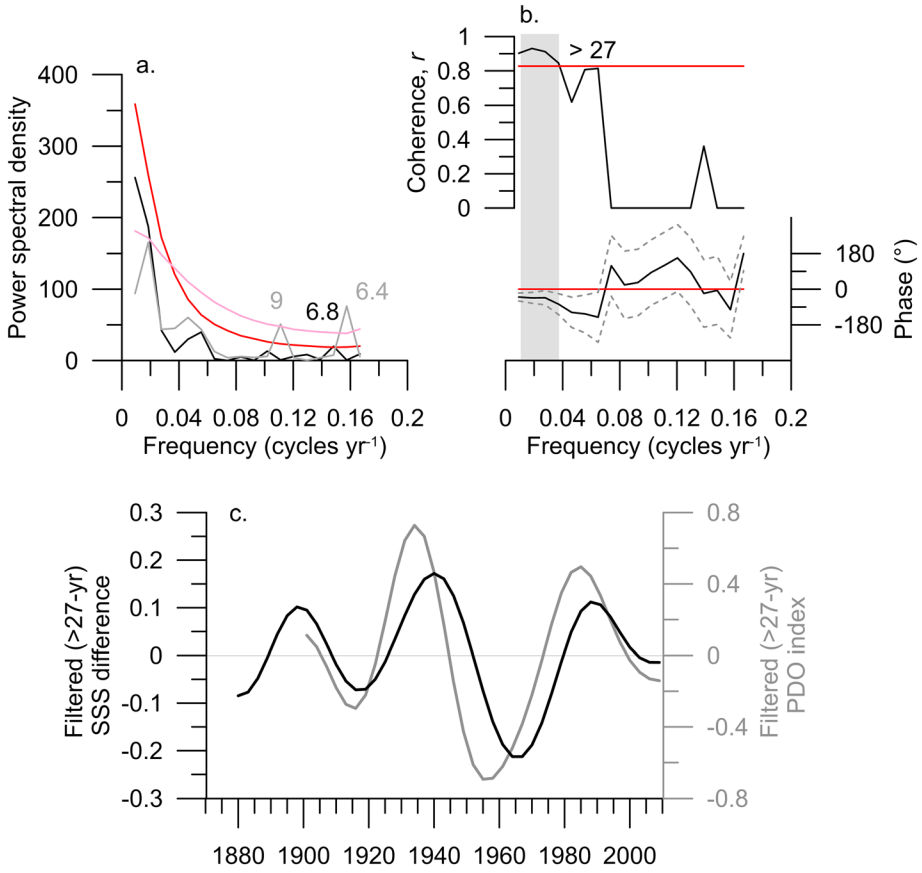

Figure 7. (a) Fast Fourier transform analysis of detrended SSS difference (black) and PDO (gray) records. Significance level greater than 90% (red line for SSS difference and pink line for PDO) are labelled. (b) Coherence multitaper method with phase analysis between records reveal significant coherence at periods >27 years. Red lines indicate 90% significance level while the gray dashed lines represent confidence intervals. (c) Filtered (>27 years) SSS difference (black) and PDO (gray) records with a 6-year PDO lead. SSS = sea surface salinity; PDO = Pacific Decadal Oscillation.

detected (Deser et al., 2004; Trenberth et al., 1998). Therefore, the significant difference between the dry and wet season salinity records during predominantly positive PDO phases is likely due to the advection of high salinity waters to our site in the dry season (Figure 6b).

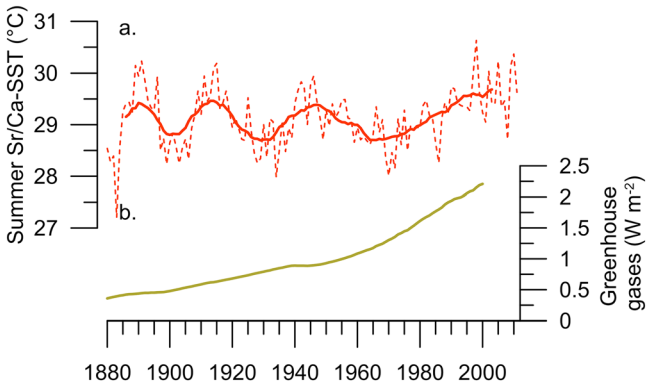

Figure 8. (a) Palaui coral-derived summer SST record (dashed red line) superimposed with 30-year moving average (solid red line) and (b) a record of well-mixed greenhouse gases (olive line; Schmidt et al., 2012). SST = sea surface temperature.

Between 1958 and 1976 when SSS difference is negligible, the dry season SSS reconstruction indicates predominance of La Niña events as previously reported (Ramos et al., 2017). La Niña-related increases in rainfall and reduced Kuroshio intrusions positively combine to decrease dry season salinity at Palaui. This period also coincides with the predominant cold PDO phase (Figure 6b), similarly reducing the Kuroshio intrusion and hindering advection of more saline waters to our site. Thus, the predominant cold PDO phase between 1958 and 1976, combined with ENSO-related freshening, lead to insignificant changes in salinity between seasons.

Overall, salinity variability at our site implies interaction between the PDO and ENSO. Warm/cold PDO and El Niño/La Niña phases constructively combine to enhance/reduce advection of more saline waters at our site. Because the PDO is viewed as a "reddened" ENSO reaction (Newman et al., 2016) where warm/cold phases are analogous to El Niño/La Niña episodes, salinity as a function of PDO-related Kuroshio water advection shows a response consistent with the

Paleoceanography and Paleoclimatology

10.1029/2019PA003684

Table 1
Correlation Between Marine and Terrestrial PDO Reconstructions

	PDO index	Ogasawara coral Sr/Ca (Felis et al., 2010) [2]	Aleutian Is. coralline algae Mg/Ca (Williams et al., 2017)[3]	Aleutian Is. coralline algae $\delta^{18}O$ (Halfar et al., 2007)[4]	N. America geoduck clam growth (Strom et al., 2004)[5]	Canada and N. America geoduck clam growth (Black et al., 2009)[6]	East Asia tree-rings (D'Arrigo & Wilson, 2006)[7]	N. America tree-rings (MacDonald & Case, 2005)[8]	N. America tree-rings (Biondi et al., 2001)[9]	Canada and N. America tree-rings (Black et al., 2009)[6]
Palaui Winter Sr/Ca-SST[1]	−0.90	−0.90	−0.87	0.93	−0.98	−0.93	−0.92	−0.39	−0.36	−0.71
PDO Index		0.97	0.66	−0.82	0.89	0.98	0.97	0.83	0.83	0.96
Ogasawara Coral Sr/Ca (Felis et al., 2010)[2]			0.59	−0.82	0.93	0.99	0.99	0.67	0.63	0.88
Aleutian Is. Coralline Algae Mg/Ca (Williams et al., 2017)[3]				−0.83	0.80	0.61	0.59	***−0.05***	*−0.12*	0.34
Aleutian Is. Coralline Algae $\delta^{18}O$ (Halfar et al., 2007)[4]					−0.92	−0.85	−0.87	−0.42	−0.41	−0.72
N. America Geoduck Clam Growth (Strom et al., 2004)[5]						0.94	0.94	0.42	0.35	0.74
Canada and N. America Geoduck Clam Growth (Black et al., 2009)[6]							1.00	0.70	0.71	0.88
East Asia Tree Rings (D'Arrigo & Wilson, 2006)[7]								0.62	0.60	0.87
N. America Tree Rings (MacDonald & Case, 2005)[8]									0.99	0.90
N. America Tree Rings (Biondi et al., 2001)[9]										0.90

Note. All numbers are significant at 95% level except those italicized. Number superscripts indicate the location of these records in supporting information Figure S6.

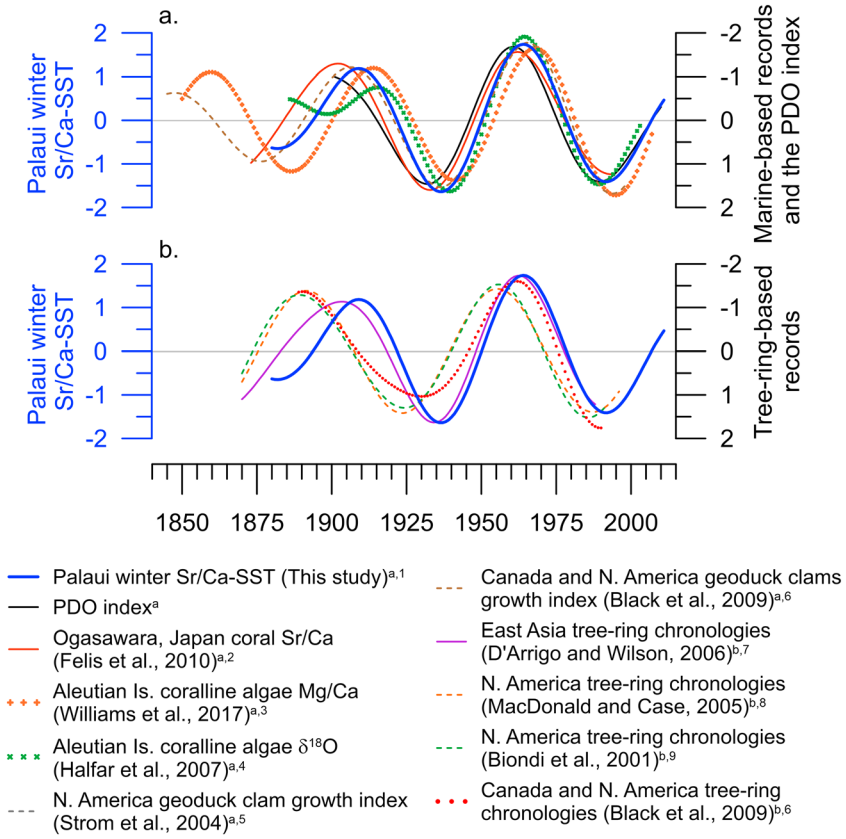

Figure 9. The 55-year filtered Palaui winter Sr/Ca-SST record compared with other (a) marine and (b) terrestrial PDO reconstructions across the Pacific. Note that the *y* axes for other PDO records were inverted to facilitate visual comparison. All timeseries were standardized by dividing each value by each of the record's standard deviation. Number superscripts in the legend indicate the location of these records in supporting information Figure S6. SST = sea surface temperature; PDO = Pacific Decadal Oscillation.

Kuroshio transport and drought/above-normal rainfall anomalies associated with El Niño/La Niña events. This suggests that the mechanisms driving ENSO-related salinity changes at our site similarly contribute to the PDO-related SSS variability.

We also compared our salinity records with previously published SSS reconstructions in close proximity to our study site—Ogasawara Island (Felis et al., 2009) in the Western Pacific and Hainan Island (Deng et al., 2013) in the northern South China Sea. These records show significant freshening trends since the late nineteenth century, though with variable magnitude and timing. In Ogasawara, the abrupt freshening in the early 1990s by as much as 0.35‰ or 0.82psu is attributed to a combined forcing of atmospheric changes and oceanic advection (Felis et al., 2009). Weakened westerlies together with reduced Kuroshio transport lead to pronounced freshening during this period. In contrast, a gradual freshening trend of ~0.4‰ since 1900 is observed in Hainan, northern South China Sea, which is attributed to PDO-related changes in rainfall over South China and terrestrial runoff (Deng et al., 2013). In Palaui, our dry season salinity record shows a similar freshening trend of 0.4‰ (0.39 psu) since the late 1800s. While the PDO impact on Hainan and Palaui records is evident, the mechanisms by which the PDO affects climate patterns at these sites are variable even within the same regional geographic location. Thus, isolating the PDO's role in the overall freshening trend remains complex. This is expected due to the numerous atmospheric and oceanic processes involved in the PDO; hence, distinguishing PDO-related impacts is critical. In Palaui, reconstructing salinity variability in different seasons presented a unique opportunity to distinguish the PDO's specific influence on changing salinity through time.

5. Conclusions

Century-long records of Sr/Ca and $\delta^{18}O$ from Palaui allow reconstruction of SST and SSS variability and evaluation of their climatic drivers. Our SST records capture significant variability, with the summer and winter records exhibiting different climate sensitivities. The summer SST record provides evidence of significant warming that commenced in the 1970s. This warming is likely tied to the rise in western Pacific SSTs associated with greenhouse warming. Our winter SST, on the other hand, is sensitive to interannual to multidecadal scale changes driven by the EAWM and the PDO, which potentially slows down the effects of anthropogenic warming. Similar to other terrestrial and marine-based PDO records across the Pacific, our record exhibits decadal climate variability strongly correlated to the PDO. Comparing PDO records from the western, northern, and eastern Pacific yields reduced correlation across basins, which may indicate a change in the spatial pattern of the PDO. Because the PDO and EAWM affect SST at our site in a similar direction, the dominance of PDO-related changes in our winter SST record obscures the monsoonal impact. However, these interrelationships through time may provide clues on the reversing roles of the PDO and EAWM in modulating winter SSTs at high frequencies.

Reconstructing salinity variability at different seasons similarly allowed for identifying distinct salinity controls between the wet and dry seasons. Both ENSO and non-ENSO-related rainfall patterns are evident in our salinity records. By determining the seasonal salinity difference through time, the PDO's control on salinity in this region is additionally revealed. The PDO and ENSO constructively combine to enhance/reduce advection of more saline Kuroshio waters to our site.

Overall, this study demonstrates that climate records from a tropical reef environment like Palaui robustly capture PDO variability and related changes over a century. The strong imprint of decadal variability potentially masks the effects of anthropogenic warming and maintains a stable-appearing long-term mean SST. This also implies that the tropical western Pacific is a key region for understanding multi-frequency climate variability throughout the Pacific basin, including changing patterns of impact on tropical climate at longer timescales.

Acknowledgments
The authors would like to thank J. Ossolinski, J. Aggangan, J. Quevedo, R. Lloren, G. Albano, J. Perez, and A. Bolton for their help in acquiring core samples in the field. The detailed comments and suggestions of two anonymous reviewers significantly improved the original manuscript. This research was funded by the National Research Foundation Singapore under its Singapore NRF Fellowship scheme awarded to N. F. Goodkin (National Research Fellow award NRF-RF2012-03), as administered by the Earth Observatory of Singapore and the Singapore Ministry of Education under the Research Centers of Excellence initiative and by the Ministry of Education, Singapore through its Academic Research Fund Tier 2 (Project MOE2016-T2-1-016). The coral Sr/Ca and $\delta^{18}O$ data generated in this study are available in the supporting information Data Set S1 and are archived at the NOAA NCDC World Data Center for Paleoclimatology (https://www.ncdc.noaa.gov/paleo/study/27271). Other data and resources used in this study were sourced from the following sites: PDO index (http://research.jisao.washington.edu/pdo/PDO.latest); IPO index (https://www.esrl.noaa.gov/psd/data/timeseries/IPOTPI/ipotpi.hadisst2.data); NP index (https://www.esrl.noaa.gov/psd/data/correlation/np.data); PDO and North Pacific SST reconstructions (https://www.ncdc.noaa.gov/data-access/paleoclimatology-data); and MTM coherence and phase analysis MATLAB® code (https://www.mathworks.com/matlabcentral/fileexchange/22551-multi-taper-coherence-method-with-bias-correction).

References

Asami, R., Yamada, T., & Iryu, Y. (2005). Interannual and decadal variability of the western Pacific sea surface condition for the years 1787–2000: Reconstruction based on stable isotope record from a Guam coral. *Journal of Geophysical Research*, *110*, C05018. https://doi.org/10.1029/2004JC002555

Biondi, F., Gershunov, A., & Cayan, D. R. (2001). North Pacific Decadal Climate Variability since 1661. *Journal of Climate*, *14*(1), 5–10. https://doi.org/10.1175/1520-0442(2001)014<0005:NPDCVS>2.0.CO;2

Black, B. A., Copenheaver, C. A., Frank, D. C., Stuckey, M. J., & Kormanyos, R. E. (2009). Multi-proxy reconstructions of northeastern Pacific sea surface temperature data from trees and Pacific geoduck. *Palaeogeography, Palaeoclimatology, Palaeoecology*, *278*(1-4), 40–47. https://doi.org/10.1016/j.palaeo.2009.04.010

Carton, J. A., & Giese, B. S. (2008). A Reanalysis of Ocean Climate Using Simple Ocean Data Assimilation (SODA). *Monthly Weather Review*, *136*(8), 2999–3017. https://doi.org/10.1175/2007MWR1978.1

Cobb, K. M., Charles, C. D., & Hunter, D. E. (2001). A central tropical Pacific coral demonstrates Pacific, Indian, and Atlantic decadal climate connections. *Geophysical Research Letters*, *28*(11), 2209–2212. https://doi.org/10.1029/2001GL012919

Cole, J. E., Dunbar, R., McClanahan, T., & Muthiga, N. A. (2000). Tropical Pacific forcing of decadal SST variability in the western Indian Ocean over the past two centuries. *Science*, *287*(5453), 617–619. https://doi.org/10.1126/science.287.5453.617

D'Arrigo, R., & Wilson, R. (2006). On the Asian expression of the PDO. *International Journal of Climatology*, *26*(12), 1607–1617. https://doi.org/10.1002/joc.1326

D'Arrigo, R., Wilson, R., Panagiotopoulos, F., & Wu, B. (2005). On the long-term interannual variability of the east Asian winter monsoon. *Geophysical Research Letters*, *32*, L21706. https://doi.org/10.1029/2005GL023235

Delcroix, T., Cravatte, S., & McPhaden, M. J. (2007). Decadal variations and trends in tropical Pacific sea surface salinity since 1970. *Journal of Geophysical Research*, *112*, C03012. https://doi.org/10.1029/2006JC003801

Deng, W., Wei, G., Xie, L., Ke, T., Wang, Z., Zeng, T., & Liu, Y. (2013). Variations in the Pacific Decadal Oscillation since 1853 in a coral record from the northern South China Sea. *Journal of Geophysical Research: Oceans*, *118*, 2358–2366. https://doi.org/10.1002/jgrc.20180

Deser, C., Phillips, A. S., & Hurrell, J. W. (2004). Pacific interdecadal climate variability: Linkages between the Tropics and the North Pacific during boreal winter since 1900. *Journal of Climate*, *17*(16), 3109–3124. https://doi.org/10.1175/1520-0442(2004)017<3109:PICVLB>2.0.CO;2

Felis, T., Suzuki, A., Kuhnert, H., Dima, M., Lohmann, G., & Kawahata, H. (2009). Subtropical coral reveals abrupt early-twentieth-century freshening in the western North Pacific Ocean. *Geology*, *37*(6), 527–530. https://doi.org/10.1130/G25581A.1

Felis, T., Suzuki, A., Kuhnert, H., Rimbu, N., & Kawahata, H. (2010). Pacific Decadal Oscillation documented in a coral record of North Pacific winter temperature since 1873. *Geophysical Research Letters*, *37*, L14605. https://doi.org/10.1029/2010GL043572

Gedalof, Z. e., & Smith, D. J. (2001). Interdecadal climate variability and regime-scale shifts in Pacific North America. *Geophysical Research Letters*, *28*(8), 1515–1518. https://doi.org/10.1029/2000GL011779

Graham, N. E. (1995). Simulation of recent global temperature trends. *Science*, *267*(5198), 666–671. https://doi.org/10.1126/science.267.5198.666

Halfar, J., Steneck, R., Schöne, B., Moore, G. W. K., Joachimski, M., Kronz, A., et al. (2007). Coralline alga reveals first marine record of subarctic North Pacific climate change. *Geophysical Research Letters*, *34*, L07702. https://doi.org/10.1029/2006GL028811

Hathorne, E. C., Gagnon, A., Felis, T., Adkins, J., Asami, R., Boer, W., et al. (2013). Interlaboratory study for coral Sr/Ca and other element/Ca ratio measurements. *Geochemistry, Geophysics, Geosystems*, *14*, 3730–3750. https://doi.org/10.1002/ggge.20230

Hu, D., Wu, L., Cai, W., Gupta, A. S., Ganachaud, A., Qiu, B., et al. (2015). Pacific western boundary currents and their roles in climate. *Nature*, *522*(7556), 299–308. https://doi.org/10.1038/nature14504

Huybers, P., & Denton, G. (2008). Antarctic temperature at orbital timescales controlled by local summer duration. *Nature Geoscience*, *1*(11), 787–792. https://doi.org/10.1038/ngeo311

Kim, J.-W., Yeh, S.-W., & Chang, E.-C. (2014). Combined effect of El Niño–Southern Oscillation and Pacific Decadal Oscillation on the East Asian winter monsoon. *Climate Dynamics*, *42*(3-4), 957–971. https://doi.org/10.1007/s00382-013-1730-z

Lean, J. (2000). Evolution of the Sun's spectral irradiance since the Maunder Minimum. *Geophysical Research Letters*, *27*(16), 2425–2428. https://doi.org/10.1029/2000GL000043

Linsley, B. K., Wellington, G. M., & Schrag, D. P. (2000). Decadal sea surface temperature variability in the subtropical South Pacific from 1726 to 1997 A.D. *Science*, *290*(5494), 1145–1148. https://doi.org/10.1126/science.290.5494.1145

Liu, Z., & Di Lorenzo, E. (2018). Mechanisms and predictability of Pacific decadal variability. *Current Climate Change Reports*, *4*(2), 128–144. https://doi.org/10.1007/s40641-018-0090-5

MacDonald, G. M., & Case, R. A. (2005). Variations in the Pacific Decadal Oscillation over the past millennium. *Geophysical Research Letters*, *32*, L08703. https://doi.org/10.1029/2005GL022478

Mantua, N. J., & Hare, S. R. (2002). The Pacific Decadal Oscillation. *Journal of Oceanography*, *58*(1), 35–44. https://doi.org/10.1023/A:1015820616384

Mantua, N. J., Hare, S. R., Zhang, Y., Wallace, J., & M., & Francis, R. C. (1997). A Pacific interdecadal climate oscillation with impacts on salmon production. *Bulletin of the American Meteorological Society*, *78*(6), 1069–1079. https://doi.org/10.1175/1520-0477(1997)078<1069:APICOW>2.0.CO;2

Miller, A. J., Cayan, D. R., Barnett, T. P., Graham, N. E., & Oberhuber, J. M. (1994). The 1976–77 climate shift of the Pacific Ocean. *Oceanography*, *7*(1), 21–26. https://doi.org/10.5670/oceanog.1994.11

Minobe, S. (1997). A 50–70 year climatic oscillation over the North Pacific and North America. *Geophysical Research Letters*, *24*(6), 683–686. https://doi.org/10.1029/97GL00504

Nan, F., Xue, H., & Yu, F. (2015). Kuroshio intrusion into the South China Sea: A review. *Progress in Oceanography*, *137*, 314–333. https://doi.org/10.1016/j.pocean.2014.05.012

Newman, M., Alexander, M. A., Ault, T. R., Cobb, K. M., Deser, C., Di Lorenzo, E., et al. (2016). The Pacific Decadal Oscillation, Revisited. *Journal of Climate*, *29*(12), 4399–4427. https://doi.org/10.1175/JCLI-D-15-0508.1

Nigam, S., Barlow, M., & Berbery, E. H. (1999). Analysis links Pacific Decadal Variability to drought and streamflow in United States. *Eos, Transactions American Geophysical Union*, *80*(51), 621–625. https://doi.org/10.1029/99EO00412

Nurhati, I. S., Cobb, K. M., & Di Lorenzo, E. (2011). Decadal-scale SST and salinity variations in the central tropical Pacific: Signatures of natural and anthropogenic climate change. *Journal of Climate*, *24*(13), 3294–3308. https://doi.org/10.1175/2011JCLI3852.1

Okai, T., Suzuki, A., Kawahata, H., Terashima, S., & Imai, N. (2001). Preparation of a New Geological Survey of Japan Geochemical Reference Material: Coral JCp-1. *Geostandards Newsletter*, *26*, 95–99.

Overland, J., Rodionov, S., Minobe, S., & Bond, N. (2008). North Pacific regime shifts: Definitions, issues and recent transitions. *Progress in Oceanography*, *77*(2-3), 92–102. https://doi.org/10.1016/j.pocean.2008.03.016

Paillard, D., Labeyrie, L., & Yiou, P. (1996). Macintosh Program performs time-series analysis. *Eos, Transactions American Geophysical Union*, *77*(39), 379.

Power, S., Casey, T., Folland, C. K., Colman, A., & Mehta, V. M. (1999). Inter-decadal modulation of the impact of ENSO on Australia. *Climate Dynamics*, *15*(5), 319–324. https://doi.org/10.1007/s003820050284

Qu, T., Kim, Y. Y., & Yaremchuk, M. (2004). Can Luzon Strait transport play a role in conveying the impact of ENSO to the South China Sea? *Journal of Climate*, *17*(18), 3644–3657. https://doi.org/10.1175/1520-0442(2004)017<3644:CLSTPA>2.0.CO;2

Qu, T., Mitsudera, H., & Yamagata, T. (1998). On the western boundary currents in the Philippine Sea. *Journal of Geophysical Research*, *103*(C4), 7537–7548. https://doi.org/10.1029/98JC00263

Ramos, R. D., Goodkin, N. F., Druffel, E. R. M., Fan, T. Y., & Siringan, F. P. (2019). Interannual coral $\Delta^{14}C$ records of surface water exchange across the Luzon Strait. *Journal of Geophysical Research: Oceans*, *124*, 491–505. https://doi.org/10.1029/2018JC014735

Ramos, R. D., Goodkin, N. F., Siringan, F. P., & Hughen, K. A. (2017). Diploastrea heliopora Sr/Ca and $\delta^{18}O$ records from northeast Luzon, Philippines: An assessment of interspecies coral proxy calibrations and climate controls of sea surface temperature and salinity. *Paleoceanography*, *32*, 424–438. https://doi.org/10.1002/2017PA003098

Rayner, N. A., Parker, E. D., Horton, E. B., Folland, C. K., Alexander, L. V., Rowell, D. P., et al. (2003). Global analyses of sea surface temperature, sea ice, and night marine air temperature since the late nineteenth century. *Journal of Geophysical Research*, *108*(D14), 4407. https://doi.org/10.1029/2002JD002670

Reynolds, R. W., Rayner, N. A., Smith, T. M., Stokes, D. C., & Wang, W. (2002). An improved in situ and satellite SST analysis for climate. *Journal of Climate*, *15*(13), 1609–1625. https://doi.org/10.1175/1520-0442(2002)015<1609:AIISAS>2.0.CO;2

Schmidt, G. A., Jungclaus, J. H., Ammann, C. M., Bard, E., Bracconot, P., Crowley, T. J., et al. (2012). Climate forcing reconstructions for use in PMIP simulations of the Last Millenium (v1.1). *Geoscientific Model Development*, *5*(1), 185–191. https://doi.org/10.5194/gmd-5-185-2012

Schrag, D. P. (1999). Rapid analysis of high-precision Sr/Ca ratios in corals and other marine carbonates. *Paleoceanography*, *14*(2), 97–102. https://doi.org/10.1029/1998PA900025

Stichler, W. (1995). Interlaboratory comparison of new materials for carbon and oxygen isotope ratio measurements. Paper presented at the Reference and intercomparison materials for stable isotopes of light elements, IAEA, Vienna.

Strom, A., Francis, R. C., Mantua, N. J., Miles, E. L., & Peterson, D. L. (2004). North Pacific climate recorded in growth rings of geoduck clams: A new tool for paleoenvironmental reconstruction. *Geophysical Research Letters*, *31*, L06206. https://doi.org/10.1029/2004GL019440

Tierney, J. E., Abram, N. J., Anchukaitis, K. J., Evans, M. N., Giry, C., Kilbourne, K. H., et al. (2015). Tropical sea surface temperatures for the past four centuries reconstructed from coral archives. *Paleoceanography*, *30*, 226–252. https://doi.org/10.1002/2014PA002717

Trenberth, K. E., Branstator, G. W., Karoly, D., Kumar, A., Lau, N.-C., & Ropelewski, C. (1998). Progress during TOGA in understanding and modeling global teleconnections associated with tropical sea surface temperatures. *Journal of Geophysical Research*, *103*(C7), 14291–14324. https://doi.org/10.1029/97JC01444

Trenberth, K. E., & Hurrell, J. W. (1994). Decadal atmosphere-ocean variations in the Pacific. *Climate Dynamics*, *9*(6), 303–319. https://doi.org/10.1007/BF00204745

Urban, F. E., Cole, J. E., & Overpeck, J. T. (2000). Influence of mean climate change on climate variability from a 155-year tropical Pacific coral record. *Nature*, *407*(6807), 989–993. https://doi.org/10.1038/35039597

Wang, H., & Mehta, V. M. (2008). Decadal Variability of the Indo-Pacific warm pool and its association with atmospheric and oceanic variability in the NCEP–NCAR and SODA Reanalyses. *Journal of Climate*, *21*(21), 5545–5565. https://doi.org/10.1175/2008JCLI2049.1

Wang, L., Chen, W., & Huang, R. (2008). Interdecadal modulation of PDO on the impact of ENSO on the east Asian winter monsoon. *Geophysical Research Letters*, *35*, L20702. https://doi.org/10.1029/2008GL035287

Watanabe, T., Kawamura, T., Yamazaki, A., Murayama, M., & Yamano, H. (2014). A 106 year monthly coral record reveals that the East Asian summer monsoon modulates winter PDO variability. *Geophysical Research Letters*, *41*, 3609–3614. https://doi.org/10.1002/2014GL060037

Williams, B., Halfar, J., DeLong, K. L., Smith, E., Steneck, R., Lebednik, P. A., et al. (2017). North Pacific twentieth century decadal-scale variability is unique for the past 342 years. *Geophysical Research Letters*, *44*, 3761–3769. https://doi.org/10.1002/2017GL073138

Wu, C.-R. (2013). Interannual modulation of the Pacific Decadal Oscillation (PDO) on the low-latitude western North Pacific. *Progress in Oceanography*, *110*, 49–58. https://doi.org/10.1016/j.pocean.2012.12.001

Yan, X.-H., Ho, C.-R., Zheng, Q., & Klemas, V. (1992). Temperature and size variabilities of the western Pacific Warm Pool. *Science*, *258*(5088), 1643–1645. https://doi.org/10.1126/science.258.5088.1643